International Journal of Minerals, Metallurgy and Materials
Volume 28, Number 9, September 2021, Page 1478
https://doi.org/10.1007/s12613-020-2137-6

Recovery and regeneration of $LiFePO_4$ from spent lithium-ion batteries via a novel pretreatment process

Cheng Yang[1,2], *Jia-liang Zhang*[1,2,3], *Qian-kun Jing*[1,2], *Yu-bo Liu*[1,2], *Yong-qiang Chen*[1,2,3], *and Cheng-yan Wang*[1,2,3,4]

1) State Key Laboratory of Advanced Metallurgy, University of Science and Technology Beijing, Beijing 100083, China
2) School of Metallurgical and Ecological Engineering, University of Science and Technology Beijing, Beijing 100083, China
3) Beijing Key Laboratory of Green Recycling and Extraction of Metals, Beijing 100083, China
4) School of Metallurgy Engineering, Jiangxi University of Science and Technology, Ganzhou 341000, China
(Received: 5 May 2020; revised: 20 June 2020; accepted: 6 July 2020)

Abstract: The recycling of spent $LiFePO_4$ batteries has received extensive attention due to its environmental impact and economic benefit. In the pretreatment process of spent $LiFePO_4$ batteries, the separation of active materials and current collectors determines the difficulty of the recovery process and product quality. In this work, a facile and efficient pretreatment process is first proposed. After only freezing the electrode pieces and immersing them in boiling water, $LiFePO_4$ materials were peeled from the Al foil. Then, after roasting under an inert atmosphere and sieving, all the cathode and anode active materials were easily and efficiently separated from the Al and Cu foils. The active materials were subjected to acid leaching, and the leaching solution was further used to prepare $FePO_4$ and Li_2CO_3. Finally, the battery-grade $FePO_4$ and Li_2CO_3 were used to re-synthesize $LiFePO_4$/C via the carbon thermal reduction method. The discharge capacities of re-synthesized $LiFePO_4$/C cathode were 144.2, 139.0, 133.2, 125.5, and 110.5 $mA\cdot h\cdot g^{-1}$ at rates of 0.1, 0.5, 1, 2, and 5 C, which satisfies the requirement for middle-end $LiFePO_4$ batteries. The whole process is environmental and has great potential for industrial-scale recycling of spent lithium-ion batteries.

Keywords: spent lithium iron phosphate batteries; pretreating process; recovery; regeneration; cathode materials

1. Introduction

Olivine $LiFePO_4$ has been considered as the most potential cathode material for lithium-ion batteries (LIBs) due to its safety, low material cost, high specific capacity, and good cycling performance [1–4]. Therefore, $LiFePO_4$ batteries have been industrialized and widely applied in large vehicles or facilities; these batteries are estimated to experience a rapid increase in the next ten years [5–6]. However, the extensive consumption of $LiFePO_4$ type Li-ion power batteries means that huge numbers of spent $LiFePO_4$ batteries need to be disposed in the near future [7–8]. Scrapped $LiFePO_4$ batteries contain harmful organic electrolytes, such as dimethyl carbonate, ethyl methyl carbonate, $LiPF_6$, and heavy metals [9–12]. The proper disposal of spent $LiFePO_4$ batteries is favorable for protecting the environment and conserving resources.

At present, the recycling process of spent $LiFePO_4$ batteries mainly includes two steps: pretreatment and recovery of valuable metals. The pretreatment process mainly involves discharging, dismantling, crushing, and separation of active materials from the current collectors [13–14]. The separation process is crucial and determines the difficulty of $LiFePO_4$ recovery process and product quality. In general, three different separation processes exist: heat treatment [15–17], alkali solution dissolution [17–19], and organic solvent dissolution [17,20–21]. However, several problems impede the pretreatment process. For example, simple heat treatment cannot effectively separate active materials from current collectors, and the dissolution processes by alkali solution and organic solvents have the disadvantages of high reagent cost and generation of waste alkaline or organic solution.

The separated active materials are further treated to recover valuable metals through several methods, including direct regeneration, selective recovery of lithium, and combination method of acid leaching and synthesizing products. Direct regeneration refers to the direct repair of spent $LiFePO_4$ cathode material by supplementing lithium and high-temperature

Corresponding authors: Jia-liang Zhang E-mail: jialiangzhang@ustb.edu.cn; Cheng-yan Wang E-mail: chywang@yeah.net

Springer

treatment [22–24]. This method is widely investigated in the laboratory due to its short process flow, simple operation, and easy control. However, direct regeneration is only suitable for $LiFePO_4$ cathode scrap that contains minimal impurities and comes from one batch of spent LIBs [25]. Several methods were proposed for one-step selective leaching of lithium [7,26–28]. However, the recovered $FePO_4$ with high impurities is difficult to use when preparing $LiFePO_4$ with excellent electrochemical performance. The combination method of acid leaching and synthesizing products is the first to use a strong acid solution to completely dissolve the cathode material and extract valuable metals in the leaching solution by precipitation [29–31]. This process can achieve deep removal of impurities, and the control of morphology of synthesized $FePO_4$ materials is easily realized in the solution system. Thus, the final re-synthesized $LiFePO_4$/C materials can attain or have electrochemical properties close to those of nascent materials.

In this paper, a new pretreating method, including discharging, dismantling, freezing, immersing in boiling water, roasting in an inert atmosphere, and sieving, was applied to obtain active materials and current collectors. $FePO_4$ was obtained by the process of leaching active materials with sulfuric acid solution, oxidation precipitation, and roasting. Li_2CO_3 was recovered from the filtrate by adding saturated Na_2CO_3. Finally, $LiFePO_4$/C sample was prepared using the obtained $FePO_4$ and Li_2CO_3 via a carbon thermal reduction process.

2. Experimental

2.1. Pretreatment of spent $LiFePO_4$ batteries

Fig. 1 illustrates a flowsheet of the recycling process of spent $LiFePO_4$ batteries. For security considerations, spent $LiFePO_4$ batteries were discharged first in a 10 $g \cdot L^{-1}$ NaCl solution for 12 h. Then, the spent $LiFePO_4$ batteries were dismantled into cathode and anode electrodes, organic separators, and shell. The cathode and anode electrodes were cut into small pieces with a size of about 1.5 cm × 1.5 cm. The electrode pieces were frozen for 1 h and then immediately immersed in boiling water for 10 min. Finally, the cathode and anode electrodes were heat-treated to remove the adhesive (500°C, 2 h, and an inert atmosphere) and sieved to obtain active materials (mixed powder of $LiFePO_4$ and C) and current collectors (Al and Cu foils).

2.2. Acid leaching

Sulfuric acid was used as the leaching agent to dissolve active materials. In the acid leaching process, ascorbic acid was used as the reducing agent to reduce the oxidized Fe^{3+} in the raw materials to easily leached Fe^{2+}, and to prevents the oxidation of Fe^{2+} to Fe^{3+}. All the leaching experiments were conducted in a water bath, and the stirring speed was fixed at 500 r/min. The factors influencing the leaching efficiencies

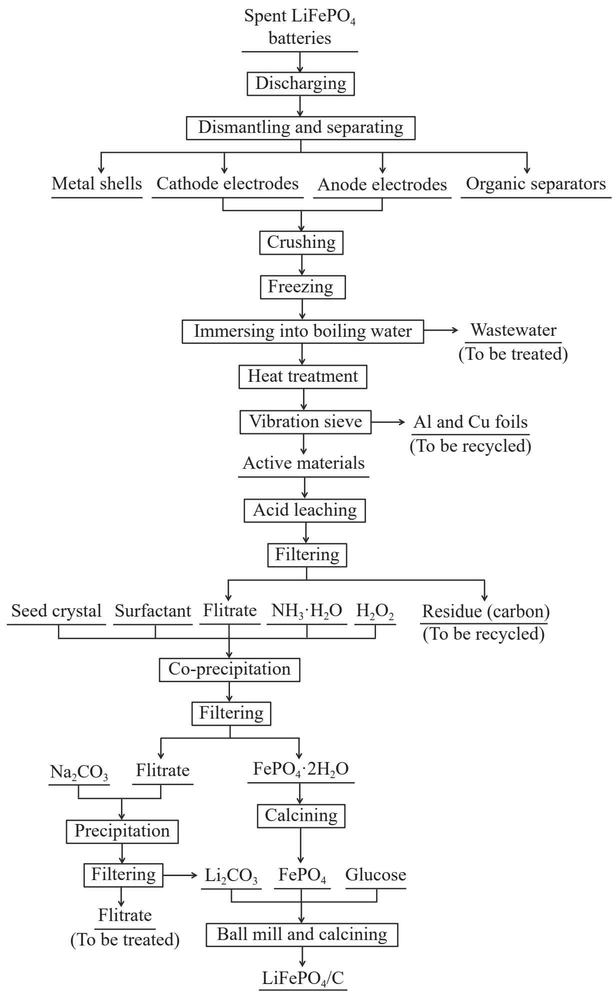

Fig. 1. Flowsheet of spent $LiFePO_4$ batteries recycling process.

of active materials were investigated; these factors included ascorbic acid dosage (0–15wt% of the mass of active materials), H_2SO_4 dosage (1.0–2.0 times of theoretical amount), reaction temperature (30–80°C), reaction time (1–5 h), and liquid-to-solid ratio (2–6 $mL \cdot g^{-1}$). The leaching efficiencies η_r of Li, Fe, and P from the active materials were calculated by using the following equation:

$$\eta_r = \frac{c_r \times V}{m_r \times \omega_r} \times 100\% \qquad (1)$$

where m_r (g) and ω_r are the mass of active materials and content of element "r" in the active material, respectively. Variables c_r ($g \cdot L^{-1}$) and V (L) are the concentration of element "r" and volume of leaching solution, respectively.

2.3. Synthesis of $FePO_4$

A certain volume of sulfuric acid solution with pH = 2.5 was first prepared as a base solution. Seed crystals of $FePO_4 \cdot 2H_2O$ and surfactant (cetrimonium bromide) were added to the base solution. The molar ratio of Fe and P was adjusted to 1.0 by adding a certain amount of $FeSO_4$ and

$(NH_4)_2HPO_4$ to the acid leachate. Then, the adjusted leaching solution and H_2O_2 solution were added to the base solution at a certain flow rate, and $NH_3·H_2O$ was simultaneously added to control the pH value at 2.5 (flow rate of acid leaching solution, 25 $mL·h^{-1}$; holding temperature, 80°C; holding time, 2 h; agitation speed, 400 $r·min^{-1}$). The suspended solution was then aged for 36 h, resulting in the growth of $FePO_4·2H_2O$ crystals. Filtration was followed, and filter cake was then added to the phosphoric acid solution to convert a small amount of $Fe(OH)_3$ to $FePO_4$ (H_3PO_4 concentration, 0.1 $mol·L^{-1}$; liquid-to-solid ratio, 10 $mL·g^{-1}$; reaction temperature, 90°C; reaction time, 2 h). Finally, the filter cake was thoroughly washed with deionized water and further dried to obtain the amorphous $FePO_4·2H_2O$. $FePO_4$ can be obtained from the amorphous $FePO_4·2H_2O$ by calcining at 600°C for 5 h.

2.4. Synthesis of Li_2CO_3

The filtrate obtained after precipitating $FePO_4·2H_2O$ was concentrated, and saturated Na_2CO_3 solution was then added to the concentrated solution at 95°C for 1 h. Finally, lithium was precipitated as Li_2CO_3, and the impurity ions remaining on the surface of the Li_2CO_3 product were washed with boiling deionized water.

2.5. Re-synthesis of $LiFePO_4$/C

A stoichiometric mixture of recovered $FePO_4$, Li_2CO_3, and glucose as carbon source (molar ratio of 2:1.03:0.4) was used to re-synthesize $LiFePO_4$/C materials via the carbon thermal reduction method. These reactants were mixed and ball-milled together for 6 h with ethanol as a dispersant. $LiFePO_4$/C materials can be obtained from the milled mixture by calcining in a N_2 atmosphere [32].

2.6. Characterization

The contents of lithium, iron, and phosphorus in the solution were measured with inductively coupled plasma optical emission spectrometry (ICP-OES, Optima 7000 DV, Perkin Elmer instruments, US). The raw materials and synthetic products were measured using X-ray diffraction (XRD, RINT-TTR3, RIGAKU, Japan), scanning electron microscopy (SEM, MLA250, FEI, US), and energy dispersive X-ray spectroscopy system (EDS, MLA250, FEI, US). The particle size of synthesized $FePO_4$ was analyzed using a laser particle size analyzer (Mastersizer 2000, Malvern, UK). The re-synthesized $LiFePO_4$/C was analyzed using Fourier transform infrared spectroscopy (FTIR, Nicolet Nexus 410, US).

3. Results and discussion

3.1. Pretreatment process

3.1.1. Separation of foil and active materials

After discharging and dismantling the spent $LiFePO_4$ batteries, two different methods were conducted to treat the cathode and anode electrodes. The first method is direct roasting in an inert atmosphere. The cathode and anode electrodes were directly roasted to remove the adhesive at 500°C for 2 h in a tubular resistance furnace, and the active materials were then obtained by sieving. In the second method, which was proposed first in this paper, the electrode scraps were frozen, immersed in boiling water, roasted in an inert atmosphere, and sieved. Fig. 2 shows the photographs and purity comparison of the active materials obtained by these methods, and Table 1 presents their chemical compositions.

As shown in Figs. 2(a) and 2(b), after direct roasting in an inert atmosphere and sieving, part of the $LiFePO_4$ materials and most of the graphite still adhered onto the Al and Cu foils. Fig. 2(c) shows that the $LiFePO_4$ materials were peeled from the Al foil only after freezing and immersing in boiling water. After roasting in an inert atmosphere and sieving, all the cathode and anode active materials were separated from the Al and Cu foils satisfactorily (Figs. 2(d) and 2(e)), respectively. Table 1 exhibits that the total content of Al and Cu in the active materials obtained by the proposed method amounted to 0.23wt%, which is lower than the 0.85wt% obtained using the first method. This finding indicates that the active material acquired by the proposed method can be used to prepare high-purity leachate, further reducing the difficulty of purifying impurities. On the other hand, the contents of Li, Fe, P, and C in the Al and Cu foils obtained by the pro-

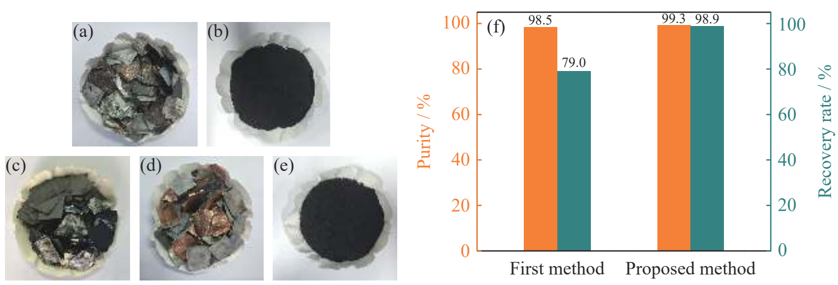

Fig. 2. Photographs of the products under different pretreatment methods: (a) Al and Cu foils and (b) active materials obtained by the first method (direct roasting and sieving); (c) cathode and anode electrodes after freezing and immersing in boiling water; (d) Al and Cu foils and (e) active materials obtained by the proposed method (freezing, immersing in boiling water, roasting, and sieving); (f) comparison of purity and recovery rate for the active materials after different pretreatment methods.

Table 1. Chemical composition of the pretreated products wt%

Method	Product	Li	Fe	P	Al	Cu	V	C
First method	Active materials	2.86	22.6	12.7	0.06	0.79	0.62	34.2
	Al and Cu foils	0.25	2.15	1.13	21.3	49.2	0.02	23.6
Proposed method	Active materials	2.15	19.4	11.1	0.05	0.18	0.51	43.9
	Al and Cu foils	0.03	0.16	0.14	32.4	66.0	0.02	1.05

posed method accounted for 1.38wt%, which is considerably lower than the 27.13wt% obtained using the first method. The results show that the proposed method can recover almost all active materials to avoid wastage of resources. Fig. 2(f) displays that compared with the first method, the proposed method can obtain active materials with purity and recovery rate higher than 98%. Thus, the proposed method can be used to separate active materials and current collectors easily and efficiently.

Fig. 3 exhibits the XRD pattern and SEM image of active materials obtained by the proposed method. The main compositions of active materials were $LiFePO_4$ and C, and no other visibly identical peaks of impurity phases were observed. All the diffraction peaks of $LiFePO_4$ can be well assigned to $LiFePO_4$ with orthorhombic olivine structure (PDF#83-2092). From the SEM image, the $LiFePO_4$ particles in the active materials were present in small spherical morphologies along with large number of secondary particles, whereas the graphite particles were present in the form of large and irregularly shaped blocks.

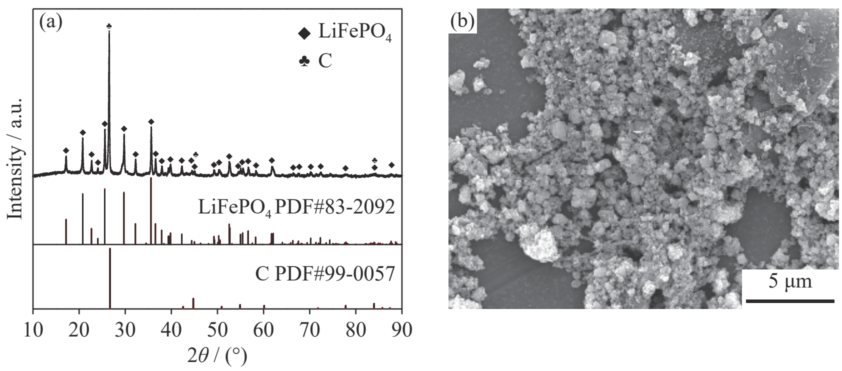

Fig. 3. (a) XRD pattern and (b) SEM image of active materials separated by the proposed pretreatment method.

3.1.2. Roasting of the active materials

The organic impurities were volatilized and removed by roasting to eliminate the effect of binder and electrolyte in the battery on product preparation. The active materials were roasted at 500°C for 2 h with or without inert gas protection. Then, the roasted products were leached with sulfuric acid solution. Fig. 4(a) shows the leaching results under the two roasting methods. After roasting with inert gas protection, the leaching efficiencies of Li, Fe, and P were 98.5%, 89.3%, and 90.3%, respectively. After roasting without inert gas protection, except for P, the leaching efficiencies of Li and Fe became notably lower. The leaching efficiencies of Li, Fe, and P were 91.4%, 70.2% and 94.8%, respectively. Figs. 4(b) and 4(c) displays the XRD results of the roasted product and corresponding leaching residue without inert gas protection. The results indicate that the main phases of the roasted product were $Li_3Fe_2(PO_4)_3$ and Fe_2O_3, and the phase of the product after acid leaching was Fe_2O_3 alone. From the thermodynam-

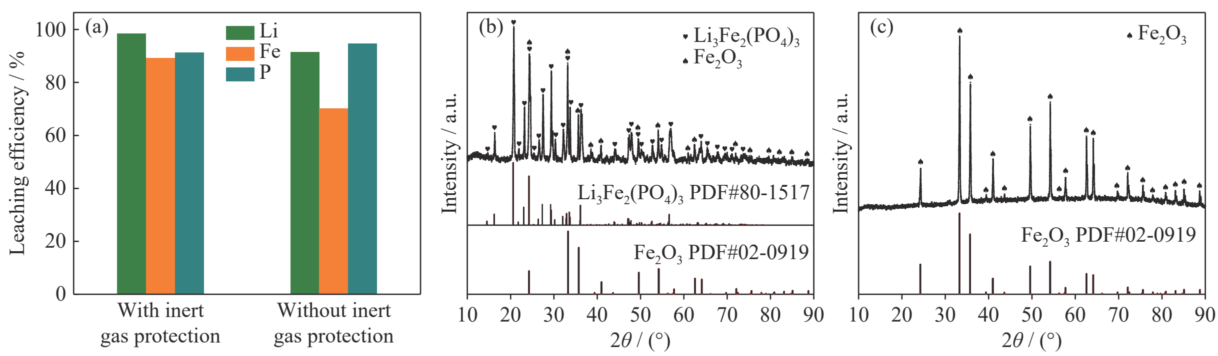

Fig. 4. (a) Comparison of leaching efficiencies of roasted products with or without inert gas protection; XRD patterns of (b) roasted product without inert gas protection and (c) corresponding acid leached product.

ic analysis of Li–Fe–P–H_2O system [33], the stable pH of $LiFePO_4$ in aqueous solution was 2−7.8. When the pH of the solution was less than 2, $LiFePO_4$ was decomposed into Li^+, Fe^{2+}, and PO_4^{3-} and dissolved in the aqueous solution. However, if Fe was present in the form of Fe^{3+} in the solution, a lower pH of the solution was required, and more acid was consumed. These findings indicate that after roasting without inert gas protection, Fe^{2+} in $LiFePO_4$ was oxidized to Fe^{3+}, and the leaching of Fe became difficult. In addition, graphite in the active materials was burned and caused wastage of resources when it was roasted without inert gas protection. Therefore, the roasting process should be carried out under vacuum or inert gas protection.

3.2. Metal leaching

3.2.1. Optimization of operating conditions

A series of experiments was carried out to obtain the optimal acid leaching conditions of active materials. The effect of mass ratio of ascorbic acid to active materials on the leaching process was investigated by maintaining H_2SO_4 dosage at twice the theoretical amount, time of 5.0 h, temperature of 80°C, and liquid-to-solid ratio of 4 mL·g^{-1}. As shown in Fig. 5(a), the leaching efficiencies of Li, Fe, and P were 98.5%, 89.3%, and 90.3% without the addition of ascorbic acid, respectively. The incomplete leaching of Fe and P may be attributed to the ferric compounds, which are more difficult to dissolve than ferrous compounds, partially contained by the active materials. When ascorbic acid was added to the solution, the leaching efficiencies of Fe and P increased significantly. When the mass ratio of ascorbic acid to active materials was increased to 3wt%, the leaching efficiencies of Li, Fe, and P increased to 99.9%, 97.5%, and 97.4%, respectively. As the mass ratio further increased, the leaching efficiencies slightly improved. Thus, the optimal mass ratio of ascorbic acid to active materials was 3wt%.

The effect of H_2SO_4 dosage on the leaching efficiencies of Li, Fe, and P was investigated by maintaining the mass ratio of ascorbic acid to active materials at 3wt%, time of 5.0 h, temperature of 80°C, and liquid-to-solid ratio at 4 mL·g^{-1}. As shown in Fig. 5(b), with the increase in H_2SO_4 dosage from 1.0 to 1.5 times of theoretical amount, the leaching efficiencies of Li, Fe, and P increased gradually. When H_2SO_4 dosage reached 1.5 times of theoretical amount, the leaching efficiencies of Li, Fe, and P were more than 98%. With the further increase in H_2SO_4 dosage, the leaching efficiencies showed no significant change and remained at a desirable level. Therefore, the best H_2SO_4 dosage for leaching is 1.5 times of theoretical amount.

The effect of leaching time on the leaching process was investigated by maintaining the mass ratio of ascorbic acid to active materials at 3wt%, H_2SO_4 dosage at 1.5 times of theoretical amount, temperature of 80°C, and liquid-to-solid ratio of 4 mL·g^{-1}. Fig. 5(c) displays that when the leaching time was 1.0 h, the leaching efficiency of Li was close to 100%, whereas the leaching efficiencies of Fe and P approximated 90%. With prolonged leaching time, the leaching efficiencies of Fe and P gradually increased. With the increase in time from 1.0 to 4.0 h, the leaching efficiencies of Li and Fe

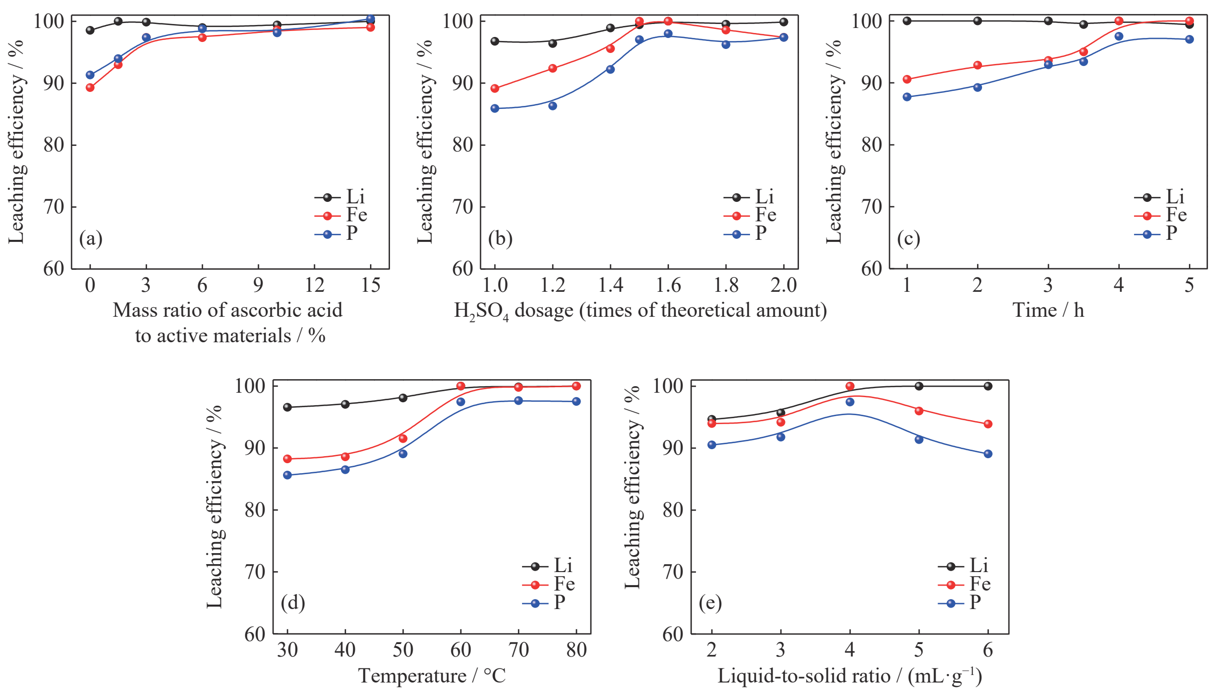

Fig. 5. Effects of various variables on the leaching process: (a) mass ratio of ascorbic acid to active materials; (b) H_2SO_4 dosage; (c) time; (d) temperature; (e) liquid-to-solid ratio.

increased from 90.6% to 99.9% and from 87.73% to 98.5%, respectively. Hence, all further experiments were carried out using 4.0 h as the optimal leaching time.

The effect of leaching temperature on the leaching process was investigated by maintaining the mass ratio of ascorbic acid to active materials at 3wt%, H_2SO_4 dosage at 1.5 times of theoretical amount, time of 4.0 h, and liquid-to-solid ratio of 4 $mL\cdot g^{-1}$. Fig. 5(d) displays that when the leaching temperature was 30°C, the leaching efficiency of Li was about 96%, whereas the leaching efficiencies of Fe and P were less than 90%. With the increase in temperature to 60°C, the leaching efficiencies of Li, Fe, and P can reach more than 98%. Therefore, 60°C is the optimal leaching temperature for acid leaching.

The effect of liquid-to-solid ratio on the leaching process was investigated by maintaining the mass ratio of ascorbic acid to active materials at 3wt%, H_2SO_4 dosage at 1.5 times of theoretical amount, time of 4.0 h, and temperature of 60°C. As shown in Fig. 5(e), the leaching efficiencies of Li, Fe, and P increased with the increase in liquid-to-solid ratio from 2 to 4 $mL\cdot g^{-1}$. When the liquid-to-solid ratio was further increased, the leaching efficiency of Li showed minimal change, and the leaching efficiencies of Fe and P slowly decreased. Evidently, 4 $mL\cdot g^{-1}$ can be considered as the optimum liquid-to-solid ratio.

3.2.2. Characterization of the leaching residue

The leaching residue was examined by SEM−EDS and XRD, and the results are presented in Fig. 6, respectively. Fig. 6(c) shows that only the identical peaks of C were observed in the XRD pattern. As depicted in Fig. 3(b) and Fig. 6(a), the morphology of the active materials changed after leaching. Fig. 6(a) shows that most of the small spherical and secondary particles disappeared, and the rest were blocky graphite particles with relatively smooth surface. In addition, EDS analysis (Fig. 6(b)) indicated that the leaching residue was mainly composed of C. The content of P was notably low, and those of Fe and V were nearly zero (Li was not detected in EDS). The characterization of the leaching residue by SEM−EDS and XRD analysis confirmed that the metals in the active materials have been efficiently extracted in the acid leaching process. The main phase of the leaching residue was unreacted graphite in the leaching process, and it can be further processed for recovery.

3.3. Characterization of recovered $FePO_4\cdot 2H_2O$ and $FePO_4$

Fe in the leaching solution was oxidized and precipitated to prepare amorphous $FePO_4\cdot 2H_2O$, whereas $FePO_4$ was further obtained from the amorphous $FePO_4\cdot 2H_2O$ by calcining at 600°C for 5 h. Fig. 7 and Table 2 show the XRD patterns of recovered $FePO_4\cdot 2H_2O$ and $FePO_4$, particle size distribution, and chemical composition of recovered $FePO_4\cdot 2H_2O$. Externally, the recovered $FePO_4\cdot 2H_2O$ and $FePO_4$ products were all light-yellow powders. Fig. 7(a) displays that the Fe and P in the solution precipitated as amorphous $FePO_4\cdot 2H_2O$. After roasting, all the diffraction peaks were well matched to

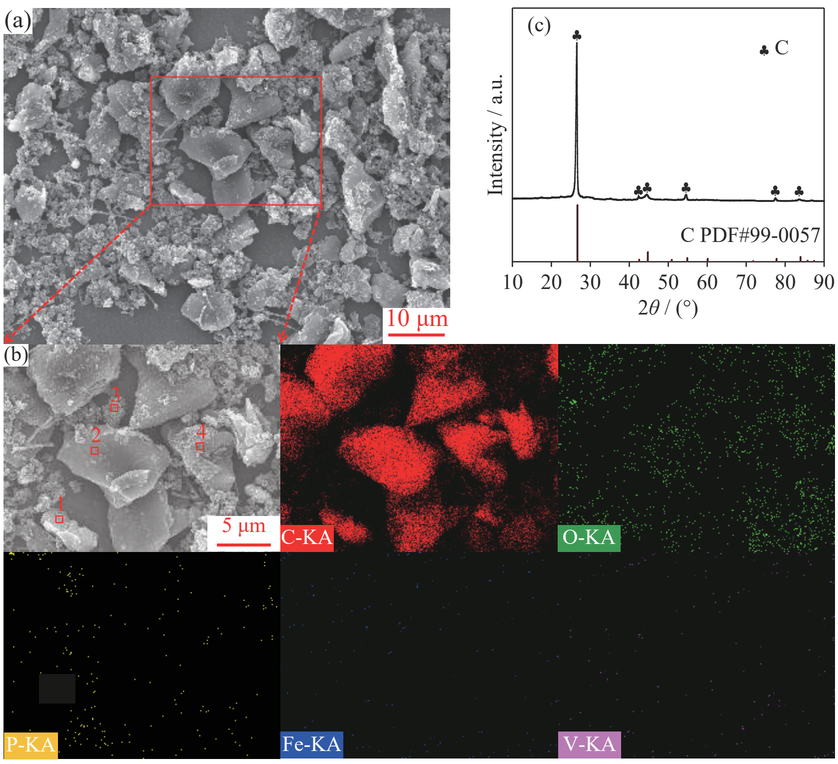

Fig. 6. SEM−EDS analyses and XRD pattern of the residue of acid leaching: (a) SEM image; (b) EDS analysis; (c) XRD pattern.

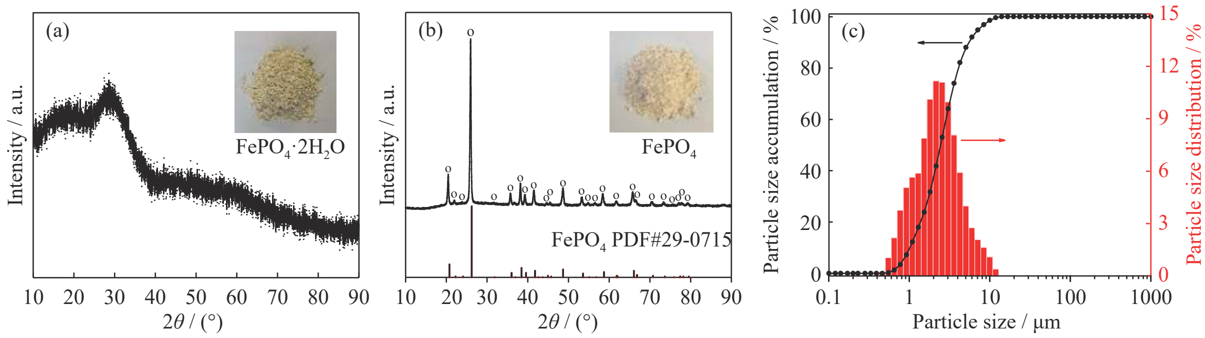

Fig. 7. XRD patterns of recovered (a) $FePO_4 \cdot 2H_2O$ and (b) $FePO_4$; (c) particle size distribution of recovered $FePO_4 \cdot 2H_2O$.

Table 2. Chemical composition of recovered $FePO_4 \cdot 2H_2O$ wt%

Fe	P	Li	Na	Al	Cu	Ca	Mg	V
29.3	16.4	<0.005	0.006	0.005	<0.005	<0.005	<0.005	<0.005

$FePO_4$, and no impurity phases were observed (Fig. 7(b)). Fig. 8 shows the SEM images of the obtained $FePO_4 \cdot 2H_2O$ and $FePO_4$. Fig. 8(a) present that the primary particles formed numerous agglomerations, which demonstrated a certain extent of irregularity. After roasting to remove water from $FePO_4 \cdot 2H_2O$, the primary particles grew and formed a nearly spherical-like shape with well uniformity; the average size of the particles was about 300–500 nm.

The main components of recovered $FePO_4 \cdot 2H_2O$ product were examined by ICP-OES. The results show that the molar ratio of Fe and P in the recovered $FePO_4 \cdot 2H_2O$ was 0.99. The contents of nearly all impurities in recovered product were extremely low. A small amount of V remained in the recovered product, and it can be used as a doping element in the cathode materials to improve the electrochemical performance of $LiFePO_4$/C [34]. The particle size distribution of recovered $FePO_4 \cdot 2H_2O$ powder was analyzed by using a laser particle size analyzer. About 80% of the powder particles were in the range of 1.0–4.5 μm, and the calculated 50% passing particle size was 2.44 μm. The component and particle size distribution of the recovered product meet the Chinese national standard of iron phosphate for batteries (HG/T 4701-2014).

3.4. Characterization of recovered Li_2CO_3

The filtrate after precipitating $FePO_4 \cdot 2H_2O$ was concentrated, and a saturated Na_2CO_3 solution was added to the concentrated solution to obtain Li_2CO_3. Fig. 9 and Table 3 show the XRD pattern, SEM image, and chemical composition of Li_2CO_3 product. The XRD pattern indicates that the white powder was Li_2CO_3, and the recovered Li_2CO_3 was highly crystalline with high purity. The SEM image revealed that the recovered Li_2CO_3 had a sheet or rod-like shape, and the particle size ranged from 2 to about 10 μm. From the ICP-OES results, the compositions of other impurities were extremely low. The purity of recovered Li_2CO_3 was 99.56wt% and met the Chinese national standard of lithium carbonate

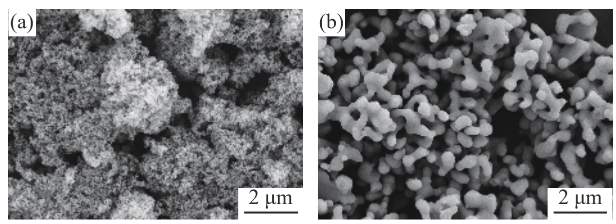

Fig. 8. SEM images of recovered (a) $FePO_4 \cdot 2H_2O$ and (b) $FePO_4$ products.

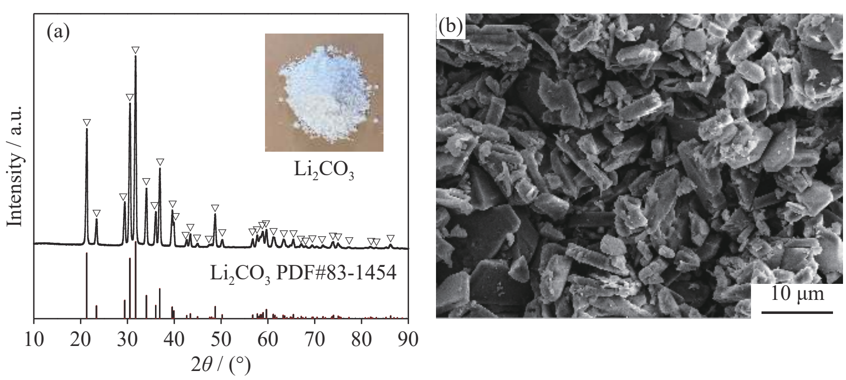

Fig. 9. (a) XRD pattern and (b) SEM image of recovered Li_2CO_3.

Table 3. Chemical composition of recovered Li_2CO_3 wt%

Li_2CO_3	P	Fe	Na	Al	Cu	Ca	Mg	V
>99.50	0.009	<0.005	<0.005	0.005	<0.005	<0.005	<0.005	<0.005

for batteries (YST 582-2013).

3.5. Characterization of re-synthesized $LiFePO_4$/C

The recovered $FePO_4$ and Li_2CO_3 can be further used to synthesize $LiFePO_4$/C materials via the carbon thermal reduction method. The crystal phase and morphology of re-synthesized $LiFePO_4$/C were investigated by XRD and SEM. All the peaks in Fig. 10(a) were assigned to orthorhombic olivine-type structure (PDF#83-2092), and no other impurity peaks were detected. From the SEM image (Fig. 10(b)), the re-synthesized $LiFePO_4$/C was composed of many sphere-like particles, and the size of sphere-like particles was in the range of 0.5−1.5 μm. Fig. 10(c) presents the FTIR spectra of commercial and re-synthesized $LiFePO_4$/C samples. Scholars have investigated and identified the IR band of $LiFePO_4$ in their earlier work [35−36]. As shown in Fig. 10(c), compared with commercial $LiFePO_4$/C, all the bands of re-synthesized $LiFePO_4$/C can be identified as intrinsic bands of $LiFePO_4$, which indicates that no impurity phases were present in the re-synthesized $LiFePO_4$/C; this finding corresponds well to the result of XRD.

Fig. 11(a) displays the cycling performances of commer-

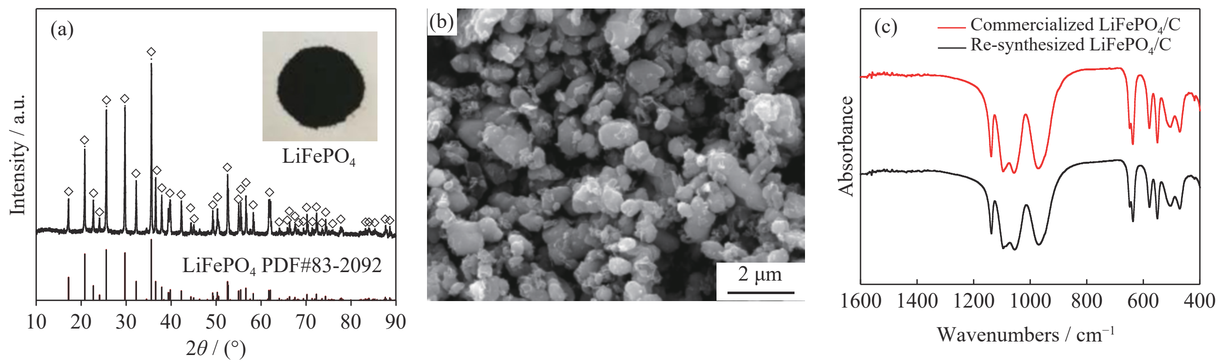

Fig. 10. (a) XRD pattern and (b) SEM image of re-synthesized $LiFePO_4$/C, and (c) FTIR spectra of commercial and re-synthesized $LiFePO_4$/C samples.

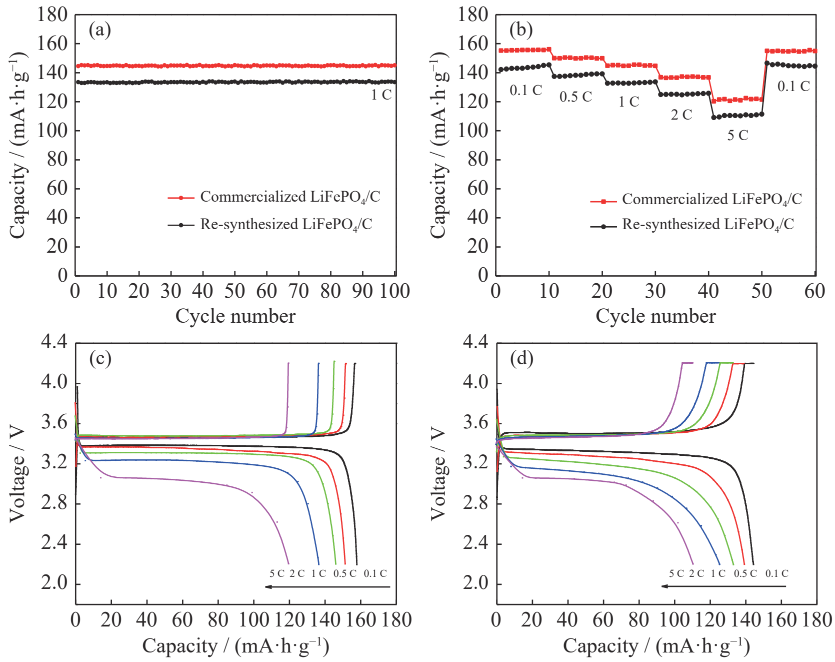

Fig. 11. Electrochemical performance of commercial and re-synthesized $LiFePO_4$/C cathodes: (a) cycling performances of both cathodes at a rate of 1 C; (b) rate capability comparison of both cathodes at various rates from 0.1 to 5 C; charge–discharge curves of (c) commercial and (d) re-synthesized $LiFePO_4$/C cathode.

cial and re-synthesized $LiFePO_4/C$ cathodes at 1 C for 100 cycles. The commercial and re-synthesized $LiFePO_4/C$ cathodes maintained capacities of 145 and 133 $mA\cdot h\cdot g^{-1}$, respectively. Both cathodes exhibited nearly 100% capacity retention, indicating that both had high capacity and excellent cycle stability. The rate performances of commercial and re-synthesized $LiFePO_4/C$ cathodes were further compared at various rates (Fig. 11(b)). As the current rate increased, the discharge capacity gradually decreased, and the discharge capacity in 10 cycles and at various rates showed no decay. Another important point is that the capacities of both cathodes were completely recovered when the current rate decreased directly from 5 to 0.1 C, indicating the high rate performances and good electrochemical reversibility.

Figs. 11(c) and 11(d) show the charge and discharge curves of commercial and re-synthesized $LiFePO_4/C$ cathodes at different rates in the voltage range of 2.2–4.3 V, respectively. The capacity of commercial $LiFePO_4/C$ cathode was a little higher than that of re-synthesized $LiFePO_4/C$ cathode. The discharge capacities of commercial $LiFePO_4/C$ cathodes were 155.2, 149.8, 144.8, 137.3, and 121.5 $mA\cdot h\cdot g^{-1}$ at rates of 0.1, 0.5, 1, 2, and 5 C, respectively. The corresponding discharge capacities of re-synthesized $LiFePO_4/C$ cathode were 144.2, 139.0, 133.2, 125.5, and 110.5 $mA\cdot h\cdot g^{-1}$, which satisfy the requirement for middle-end $LiFePO_4$ batteries (>132 $mA\cdot h\cdot g^{-1}$ at 1 C and >101 $mA\cdot h\cdot g^{-1}$ at 5 C) [23].

4. Conclusion

A facile and efficient pretreatment process has been demonstrated to recycle and re-synthesize $LiFePO_4/C$ from spent $LiFePO_4$ batteries. After freezing only the electrode pieces and immersing them in boiling water, $LiFePO_4$ materials were peeled from the Al foil. Then, after roasting in an inert atmosphere and sieving, all the cathode and anode active materials were separated from the Al and Cu foils easily and efficiently. The purity and recovery rate of active materials were higher than 98%. Under the optimized conditions, more than 98% of Li, Fe, and P can be leached from the cathode and anode active materials. Battery-grade $FePO_4$ and Li_2CO_3 can be successfully prepared, and $LiFePO_4/C$ can be further obtained by a final heat treatment. XRD and SEM analysis showed that the re-synthesized $LiFePO_4/C$ materials possessed well-crystallized and well-distributed submicron particles. Electrochemical investigation demonstrated that the discharge capacities re-synthesized $LiFePO_4/C$ cathode were 144.2, 139.0, 133.2, 125.5, and 110.5 $mA\cdot h\cdot g^{-1}$ at rates of 0.1, 0.5, 1, 2, and 5 C, which satisfy the requirements for middle-end $LiFePO_4$ batteries. This work provides a facile and efficient pretreatment method for the recovery of valuable metals from spent $LiFePO_4$ batteries.

Acknowledgements

This work was financially supported by the Key-Area Research and Development Program of Guangdong Province, China (No. 2020B090919003), the National Natural Science Foundation of China (Nos. 51834008, 51874040, and U1802253), and the Fundamental Research Funds for the Central Universities (No. FRF-TP-18-020A3).

References

[1] A. Paolella, G. Bertoni, P. Hovington, Z.M. Feng, R. Flacau, M. Prato, M. Colombo, S. Marras, L. Manna, S. Turner, G. Van Tendeloo, A. Guerfi, G.P. Demopoulos, and K. Zaghib, Cation exchange mediated elimination of the Fe-antisites in the hydrothermal synthesis of $LiFePO_4$, *Nano Energy*, 16(2015), p. 256.

[2] B.B. Wei, Y.B. Wu, F.Y. Yu, and Y.N. Zhou, Preparation and electrochemical properties of carbon-coated $LiFePO_4$ hollow nanofibers, *Int. J. Miner. Metall. Mater.*, 23(2016), No. 4, p. 474.

[3] A. Paolella, S. Turner, G. Bertoni, P. Hovington, R. Flacau, C. Boyer, Z.M. Feng, M. Colombo, S. Marras, M. Prato, L. Manna, A. Guerfi, G.P. Demopoulos, M. Armand, and K. Zaghib, Accelerated removal of Fe-antisite defects while nanosizing hydrothermal $LiFePO_4$ with Ca^{2+}, *Nano Lett.*, 16(2016), No. 4, p. 2692.

[4] A. Mauger, C. Julien, A. Paolella, M. Armand, and K. Zaghib, Building better batteries in the solid state: A review, *Materials*, 12(2019), No. 23, p. 3892.

[5] C.W. Sun, S. Rajasekhara, J.B. Goodenough, and F. Zhou, Monodisperse porous $LiFePO_4$ microspheres for a high power Li-ion battery cathode, *J. Am. Chem. Soc.*, 133(2011), No. 7, p. 2132.

[6] F. Larouche, F. Tedjar, K. Amouzegar, G. Houlachi, P. Bouchard, G.P. Demopoulos, and K. Zaghib, Progress and status of hydrometallurgical and direct recycling of Li-ion batteries and beyond, *Materials*, 13(2020), No. 3, p. 801.

[7] J.L. Zhang, J.T. Hu, Y.B. Liu, Q.K. Jing, C. Yang, Y.Q. Chen, and C.Y. Wang, Sustainable and facile method for the selective recovery of lithium from cathode scrap of spent $LiFePO_4$ batteries, *ACS Sustainable Chem. Eng.*, 7(2019), No. 6, p. 5626.

[8] Y.X. Yang, X.H. Zheng, H.B. Cao, C.L. Zhao, X. Lin, P.G. Ning, Y. Zhang, W. Jin, and Z. Sun, A closed-loop process for selective metal recovery from spent lithium iron phosphate batteries through mechanochemical activation, *ACS Sustainable Chem. Eng.*, 5(2017), No. 11, p. 9972.

[9] Q.F. Sun, X.L. Li, H.Z. Zhang, D.W. Song, X.X. Shi, J.S. Song, C.L. Li, and L.Q. Zhang, Resynthesizing $LiFePO_4/C$ materials from the recycled cathode via a green full-solid route, *J. Alloys Compd.*, 818(2020), art. No. 153292.

[10] A. Mauger, C.M. Julien, A. Paolella, M. Armand, and K. Zaghib, A comprehensive review of lithium salts and beyond for rechargeable batteries: Progress and perspectives, *Mater. Sci. Eng., R*, 134(2018), p. 1.

[11] J.L. Zhang, J.T. Hu, W.J. Zhang, Y.Q. Chen, and C.Y. Wang, Efficient and economical recovery of lithium, cobalt, nickel, manganese from cathode scrap of spent lithium-ion batteries, *J. Cleaner Prod.*, 204(2018), p. 437.

[12] H. Setiawan, H. Petrus, and I. Perdana, Reaction kinetics modeling for lithium and cobalt recovery from spent lithium-ion

batteries using acetic acid, *Int. J. Miner., Metall. Mater.*, 26(2019), No. 1, p. 98.

[13] Y.L. Yao, M.Y. Zhu, Z. Zhao, B.H. Tong, Y.Q. Fan, and Z.S. Hua, Hydrometallurgical processes for recycling spent lithium-ion batteries: a critical review, *ACS Sustainable Chem. Eng.*, 6(2018), No. 11, p. 13611.

[14] W.Q. Wang, Y.C. Zhang, L. Zhang, and S.M. Xu, Cleaner recycling of cathode material by in-situ thermite reduction, *J. Cleaner Prod.*, 249(2020), art. No. 119340.

[15] L. Sun and K.Q. Qiu, Vacuum pyrolysis and hydrometallurgical process for the recovery of valuable metals from spent lithium-ion batteries, *J. Hazard. Mater.*, 194(2011), p. 378.

[16] Y. Yang, G.Y. Huang, S.M. Xu, Y.H. He, and X. Liu, Thermal treatment process for the recovery of valuable metals from spent lithium-ion batteries, *Hydrometallurgy*, 165(2016), p. 390.

[17] X.X. Zhang, Q. Xue, L. Li, E. Fan, F. Wu, and R.J. Chen, Sustainable recycling and regeneration of cathode scraps from industrial production of lithium-ion batteries, *ACS Sustainable Chem. Eng.*, 4(2016), No. 12, p. 7041.

[18] L. Chen, X.C. Tang, Y. Zhang, L.X. Li, Z.W. Zeng, and Y. Zhang, Process for the recovery of cobalt oxalate from spent lithium-ion batteries, *Hydrometallurgy*, 108(2011), No. 1-2, p. 80.

[19] D.A. Ferreira, L.M.Z. Prados, D. Majuste, and M.B. Mansur, Hydrometallurgical separation of aluminium, cobalt, copper and lithium from spent Li-ion batteries, *J. Power Sources*, 187(2009), No. 1, p. 238.

[20] L. Li, J. Lu, Y. Ren, X.X. Zhang, R.J. Chen, F. Wu, and K. Amine, Ascorbic-acid-assisted recovery of cobalt and lithium from spent Li-ion batteries, *J. Power Sources*, 218(2012), p. 21.

[21] L. Li, R. Chen, F. Sun, F. Wu, and J.R. Liu, Preparation of $LiCoO_2$ films from spent lithium-ion batteries by a combined recycling process, *Hydrometallurgy*, 108(2011), No. 3-4, p. 220.

[22] J.P. Chen, Q.W. Li, J.S. Song, D.W. Song, L.Q. Zhang, and X.X. Shi, Environmentally friendly recycling and effective repairing of cathode powders from spent $LiFePO_4$ batteries, *Green Chem.*, 18(2016), No. 8, p. 2500.

[23] X.L. Li, J. Zhang, D.W. Song, J.S. Song, and L.Q. Zhang, Direct regeneration of recycled cathode material mixture from scrapped $LiFePO_4$ batteries, *J. Power Sources*, 345(2017), p. 78.

[24] W. Wang and Y.F. Wu, An overview of recycling and treatment of spent $LiFePO_4$ batteries in China, *Resour. Conserv. Recycl.*, 127(2017), p. 233.

[25] X. Song, T. Hu, C. Liang, H.L. Long, L. Zhou, W. Song, L. You, Z.S. Wu, and J.W. Liu, Direct regeneration of cathode materials from spent lithium iron phosphate batteries using a solid phase sintering method, *RSC Adv.*, 7(2017), No. 8, p. 4783.

[26] J.Z. Yu, X. Wang, M.Y. Zhou, and Q. Wang, A redox targeting-based material recycling strategy for spent lithium ion batteries, *Energy Environ. Sci.*, 12(2019), No. 9, p. 2672.

[27] Y. Dai, Z.D. Xu, D. Hua, H.N. Gu, and N. Wang, Theoretical-molar Fe^{3+} recovering lithium from spent $LiFePO_4$ batteries: an acid-free, efficient, and selective process, *J. Hazard. Mater.*, 396(2020), art. No. 122707.

[28] Y.X. Yang, X.Q. Meng, H.B. Cao, X. Lin, C.M. Liu, Y. Sun, Y. Zhang, and Z. Sun, Selective recovery of lithium from spent lithium iron phosphate batteries: a sustainable process, *Green Chem.*, 20(2018), No. 13, p. 3121.

[29] D.C. Bian, Y.H. Sun, S. Li, Y. Tian, Z.H. Yang, X.M. Fan, and W.X. Zhang, A novel process to recycle spent $LiFePO_4$ for synthesizing $LiFePO_4$/C hierarchical microflowers, *Electrochim. Acta*, 190(2016), p. 134.

[30] X. Wang, X.Y. Wang, R. Zhang, Y. Wang, and H.B. Shu, Hydrothermal preparation and performance of $LiFePO_4$ by using Li_3PO_4 recovered from spent cathode scraps as Li source, *Waste Manage.*, 78(2018), p. 208.

[31] R.J. Zheng, L. Zhao, W.H. Wang, Y.L. Liu, Q.X. Ma, D.Y. Mu, R.H. Li, and C.S. Dai, Optimized Li and Fe recovery from spent lithium-ion batteries via a solution-precipitation method, *RSC Adv.*, 6(2016), No. 49, p. 43613.

[32] D. Zhou, X.C. Qiu, F. Liang, S. Cao, Y.C. Yao, X.P. Huang, W.H. Ma, B. Yang, and Y.N. Dai, Comparison of the effects of $FePO_4$ and $FePO_4 \cdot 2H_2O$ as precursors on the electrochemical performances of $LiFePO_4$/C, *Ceram. Int.*, 43(2017), No. 16, p. 13254.

[33] Q.K. Jing, J.L. Zhang, Y.B. Liu, C. Yang, B.Z. Ma, Y.Q. Chen, and C.Y. Wang, E-pH diagrams for the Li−Fe−P−H_2O system from 298 to 473 K: Thermodynamic analysis and application to the wet chemical processes of the $LiFePO_4$ cathode material, *J. Phys. Chem. C*, 123(2019), No. 23, p. 14207.

[34] B. Xu, P. Dong, J.G. Duan, D. Wang, X.S. Huang, and Y.J. Zhang, Regenerating the used $LiFePO_4$ to high performance cathode via mechanochemical activation assisted V^{5+} doping, *Ceram. Int.*, 45(2019), No. 9, p. 11792.

[35] A.A. Salah, P. Jozwiak, J. Garbarczyk, K. Benkhouja, K. Zaghib, F. Gendron, and C.M. Julien, Local structure and redox energies of lithium phosphates with olivine-and Nasicon-like structures, *J. Power Sources*, 140(2005), No. 2, p. 370.

[36] C.M. Burba and R. Frech, Raman and FTIR spectroscopic study of Li_xFePO_4 ($0 \le x \le 1$) , *J. Electrochem. Soc.*, 151(2004), No. 7, p. A1032.